ANL/ET/CP-93503

RECEIVED
JUN 20 1997
OSTI

CONF-971098--

Fourth Combined Japan-US - International Energy Agency Specialists' Workshop on CERAMIC BREEDER BLANKET INTERACTIONS

October 9-11, 1995

Kyodai-kaikan, Kyoto University, Kyoto, Japan

Organizers:
Chairman M. Yamawaki (University of Tokyo)
K. Noda (JAERI)
Co-chairs: C. E. Johnson (ANL)
N. Roux (CE/SACLAY)

Local Comittee:
H. Moriyama (Kyoto University)
K. Noda (JAERI)
T. Tanabe (Nagoya University)
K. Yamaguchi (University of Tokyo)
M. Yamawaki (University of Tokyo)

MASTER

DISTRIBUTION OF THIS DOCUMENT IS UNLIMITED

DISCLAIMER

Portions of this document may be illegible in electronic image products. Images are produced from the best available original document.

DISCLAIMER

This report was prepared as an account of work sponsored by an agency of the United States Government. Neither the United States Government nor any agency thereof, nor any of their employees, make any warranty, express or implied, or assumes any legal liability or responsibility for the accuracy, completeness, or usefulness of any information, apparatus, product, or process disclosed, or represents that its use would not infringe privately owned rights. Reference herein to any specific commercial product, process, or service by trade name, trademark, manufacturer, or otherwise does not necessarily constitute or imply its endorsement, recommendation, or favoring by the United States Government or any agency thereof. The views and opinions of authors expressed herein do not necessarily state or reflect those of the United States Government or any agency thereof.

Thermal Conductivity and Tritium Retention in Li_2O and Li_2ZrO_3*

M. C. Billone
Fusion Power Program
Energy Technology and Technology Development Divisions
Argonne National Laboratory
Argonne, IL 60439 USA

Abstract

Lithium oxide (Li_2O) and lithium zirconate (Li_2ZrO_3) are promising ceramic breeder materials for fusion reactor blankets. The thermal and tritium transport databases for these materials are reviewed. Algorithms are presented for predicting both the temperature distribution and the retained tritium profile across sintered-product and pebble-bed regions. Sample design calculations are also performed to demonstrate the relative advantages of each breeder ceramic.

For Li_2O, the thermal conductivity of sintered-product material has been measured over a wide range of temperatures and densities. Data are also available for the effective thermal conductivity of a pebble bed (in atmospheric helium) with 55% packing fraction for the 5-mm-diameter/75%-dense pebbles. Similar results are available for sintered-product and pebble-bed (60% packing fraction for 1.2-mm-diameter/80%-dense pebbles in atmospheric He) Li_2ZrO_3. Hall and Martin model predictions are in reasonable agreement with both sets of pebble bed data. Thus, the databases and calculational algorithms are well established for performing thermal analyses.

Laboratory data for tritium behavior in Li_2O are available for diffusion, desorption, adsorption and solubility, as well as the critical temperatures and moisture pressures for LiOH precipitation. These data have been used to determine the model parameters in the steady-state TIARA code. In addition, TIARA has been validated to 20 data points from in-reactor, purge-flow tests after which tritium inventory measurements were obtained directly for samples irradiated at 495 - 1000°C. The database for individual rate mechanisms in Li_2ZrO_3 is less complete. However, it has been observed that the Li_2ZrO_3/H_2O system is less likely to result in LiOH precipitation in the temperature ranges of interest. Rather than use a TIARA-type approach (which requires data for individual mechanisms), a more straightforward algorithm is proposed for calculating tritium inventory in Li_2ZrO_3 based on the 31 inventory data points obtained after in-reactor purge-flow tests at 315 - 1000°C. A reasonable upper-bound fit to these data normalized to the tritium generation rate is obtained vs. temperature. This inventory/generation-rate (i.e., residency time) correlation can be used directly to bound the tritium inventory in blanket designs. The major uncertainty in this approach is in the extrapolation to temperatures below the database. Results of design calculations for each of these ceramics are presented

*Work supported by the United States Department of Energy/Office of Fusion Energy, under Contract No. W-31-109-Eng-38.

Introduction

Lithium oxide (Li_2O) is an attractive ceramic breeder material because of its high lithium atom density for tritium breeding, high thermal conductivity, good tritium release properties and low activation. However, at temperatures below a moisture-pressure-dependent critical value (e.g., 366°C at 10 Pa), LiOT/LiOH will precipitate out as a separate phase, thereby increasing tritium retention to unacceptable levels. At high temperatures (e.g., 800-1000°C), transport of vapor phase LiOT/LiOH, as well as chemical incompatibility with structural materials, may cause design problems. Thus, controling moisture pressure is essential to Li2O performance.

Lithium zirconate (Li_2ZrO_3), while not as attractive as Li_2O with regard to breeding, heat transport, and activation, has the advantage of being a more practical engineering material for large scale production, handling and blanket operation because of its stability. It also exhibits low tritium retention at low operating temperatures. Its performance in the areas of compatibility and stability (chemical, irradiation, and microstructural) is at least as good as the other ternaries (Li_4SiO_4 and $LiAlO_2$) and much better than that of Li_2O.

In the current work, algorithms are presented and validated to data for calculating temperature and tritium-retention profiles across Li_2O and Li_2ZrO_3 breeder zones. Results are presented for an ITER/EDA breeding blanket design concept.

Thermal Performance

Takahashi and Kikuchi [1] have measured the thermal conductivity [k in W $(m\ K)^{-1}$] of Li_2O in vacuum in the temperature range of $473 \le T \le 1173$ K and the porosity range of $0.066 \le p \le 0.292$. A good correlation to the data is

$$k = (1 - p)^{1.96} [39.79\ (1 + 7.067X10^{-3}\ T)^{-1}] \qquad (1)$$

Gierszewski [2] has summarized the thermal conductivity data for Li_2ZrO_3 in He in the temperature range of $373 \le T \le 1063$ K and porosity range of $0.187 \le p \le 0.211$. The data correlate well with

$$k = (1 - p)^{(5/3)} [3.643\ (1 + 1.549x10^{-3}\ T)^{-1} + 7.579x10^{-10}\ T^3] \qquad (2)$$

The Hall and Martin [3] model for the effective thermal conductivity (k_{eff}) of a single-size pebble bed is summarized by Billone et al. [4] and validated to data for Li_2O (Yoshida [5]), Li_4SiO_4 (Dalle Donne and Sordon [6]) and Li_2ZrO_3 (Sullivan et al. [7]) pebble beds in atmospheric helium. Hall and Martin derived the model for a cubic lattice of spheres with a theoretical packing fraction of 52.4%. In comparing the predictions of the k_{eff} model to data for packing fractions of 55 - 62%, particle sizes from 0.5 - 5.0 mm, and temperatures in the range of 52 - 613°C, it was found that the radiation term, which increases linearly with particle diameter, should by limited by the value corresponding to 1 mm diameter and that k_{eff} scales with packing fraction (in absolute units) as 1.26 P_f. The modified model is shown in Fig. 1 to have good agreement with the data.

A set of reference densities and configurations is established for design calculations presented in this work: an 87%-dense sintered product; a single-size pebble bed composed of coarse (0.75 mm diameter) pebbles (87% dense) at 60% packing fraction

and a net smear density of 52.2%; and a binary bed composed of the same packing fraction of coarse particles and 20% packing of fine (0.25 mm diameter) particles with a net smear density of 69.6%.

The thermal conductivities of 87% dense Li_2O and Li_2ZrO_3 are compared in Fig. 2 as functions of temperature. Also shown in Fig. 2 is the conductivity for these materials at a sintered density of 69.6%. This result sets the upper limit on the k_{eff} for the reference binary bed. The k_{eff} values for the reference single-size pebble beds are also shown. The decrease in effective conductivity from an 87% sintered product to a single-size pebble bed with 52.2% smear density is more significant for Li_2O than for Li_2ZrO_3. On the average, the Li_2O pebble-bed k_{eff} is only 1.45 times higher than that of the Li_2ZrO_3 pebble bed, as compared to a factor of 3 for the sintered-product form. Thus, there is relatively little thermal performance penalty for pebble-bed vs. sintered-product Li_2ZrO_3, while there is a much larger penalty for pebble-bed vs. sintered-product Li_2O. These calculations assume no significant source of external contact pressure on the pebble beds.

For the reference binary bed (69.6% smear density), the enhancement in k_{eff} over the single-size bed is a factor of < 2. For Li_2ZrO_3, the binary bed can enhance the single-size- bed k_{eff} by a factor of < 1.28, based on the equivalent-density sintered-product upper bound. A more sophisticated model is needed to perform the detailed binary bed calculation. For low-conductivity Li_2ZrO_3, there is relatively little gain in effective conductivity from a single-size bed to a binary bed.

Tritium Retention

Laboratory data for tritium behavior in Li_2O are available for diffusion, desorption, adsorption, solubility and LiOT/LiOH precipitation. As described by Billone [8,9], these data have been used to determine the model parameters in the steady-state TIARA code. In addition, TIARA has been validated to 20 data points from in-reactor, purge-flow tests after which tritium inventory measurements were obtained directly. A residency-time-correlation approach is also developed in the following and compared to the inventory data and the TIARA predictions. The purpose of this exercise is to learn more about the relative strengths and weaknesses of this approach for a material which has a well-developed data base and modeling code. The residency-time approach is then used to model tritium retention in Li_2ZrO_3 for which there are 31 inventory data points, but very little fundamental data.

The tritium residency time (τ, in hours) is the steady-state inventory (I in wppm) divided by the steady-state generation rate (g in wppm/hour). The residency time is related to the temperature of the breeder by a correlation which is what would be derived from a diffusion or a first-order surface desorption model:

$$\tau = \exp [A - Q/(RT)] \qquad (3)$$

where A and Q are empirically-determined parameters, $R = 8.314 \times 10^{-3}$ kJ•mole^{-1}•K^{-1} and T is temperature in K. The parameters A and Q are determined by a two-step process. Approximate values (A', Q') are first determined from an Arrhenius plot of the data for (I/g) vs. the inverse of volume-averaged temperature (T_{ave}) for the samples by

matching the calculated $\tau(T_{ave})$ to the measured I/g. However, the algorithm $I = g \bullet \tau_{ave}$, where τ_{ave} is the spatial average (determined by integration) of Eq. 3 across the breeder region, is recommended for design calculations Thus, A' and Q' are refined to give A and Q for Eq. 3 by matching $g \bullet \tau_{ave}$ to the measured values for I.

Figure 3 summarizes the measured I/g vs. the inverse of T_{ave} (515 - 955°C) for the Li_2O samples used in the EXOTIC-2, SIBELIUS, VOM-15H, CRITIC-1 and BEATRIX-II in-reactor purge flow tests. The inventory data are divided into two categories: the reference conditions of He + 0.1% H_2 purge and as-fabricated densities in the range of 80 to 86%, which are believed to be optimum from a tritium inventory point of view; and higher densities and/or lower protium contents, both of which tend to result in higher tritium inventories than the reference conditions. Also shown in Fig. 3 are the residency times deduced from the tritium release rate data in the MOZART experiment. These data have a higher source of error and are not considered as reliable as the direct inventory data. The solid line in Fig. 3 is a reasonable upper bound of the reference-condition data and corresponds to Eq. 3 with A' = -8.45 and Q' = 56. These values also give good agreement between the calculated values of $g \bullet \tau_{ave}$ and the measured values of I. Thus, A = A' = -8.45 and Q = Q' = 56 for this data set which includes local breeder temperatures in the range of 494-1000°C.

The use of Eq. 3 in the algorithm $I = g \bullet \tau_{ave}$ should yield a reasonable upper bound prediction for the tritium inventory within the fabrication (80-86% dense) and operation ($\geq$ 0.1% H_2 in the purge, T $\geq$ 494°C and g = 3.4-33.0 wppm/day) ranges of the database. The major uncertainty in using the correlation is in the extrapolation to temperatures lower than 494°C. Depending on the moisture pressure in the purge, additional inventory may be accumulated (as LiOT) if the temperature drops below a critical value: 368°C for 10.7 Pa, 328°C for 2.14 Pa and 312°C for 1.07 Pa. Also, based on desorption data and TIARA models, the single effective activation energy in the residency time approach would result in an under-prediction of inventory for T < 471°C, at which temperature the desorption activation energy increases.

The TIARA code has been validated to the inventory data base shown in Fig. 3 and the individual models in TIARA have been validated to a wide database: diffusion (300-900°C), desorption (256-653°C and ~0-5000 Pa of H_2), hydrogen solubility for Li_2O/H_2O (512-1000°C and 2-106 Pa of H_2O), hydrogen solubility for Li_2O/H_2 (400-670°C and 17-500 Pa H_2), and precipitation for Li_2O/H_2O (300-617°C and 0-1250 Pa H_2O). Thus, there is more confidence in using TIARA to calculate tritium inventory for T < 494°C, for microstructure and purge-protium contents different from the reference conditions and for design cases in which the moisture level is significant with respect to either solubility or precipitation.

Tritium inventory data are available for Li_2ZrO_3 irradiated in the EXOTIC-3,4,5,6 tests (11 data points) as reported by Kwast [10] the SIBELIUS test (1 data point) as reported by Kopasz and Johnson [11] and the BEATRIX-II (Phase II) pebble-bed test (19 data points) as reported by Verrall [12]. The measured inventories for Li_2ZrO_3, normalized to the tritium generation rate, are shown in Fig. 4, along with the residency times determined from the MOZART tritium release data. The horizontal axis represents the average temperature (360 - 1001°C) for the sample region in which the inventory was

measured. The solid line in Fig. 4 is a reasonable upper bound to the data and is given by Eq. 3 with A' = -7.0282 and Q' = 48.94. The values of these parameters are then refined based on the inventory data and the $I = g \cdot \tau_{ave}$ calculational methodology to give A = -7.7213 and Q = 50.75. The use of Eq. 3 with these coefficients gives a reasonable upper-bound prediction for tritium inventory for the local temperature range (315-1044°C) of the database. While most of the densities for the Li_2ZrO_3 experimental samples are 73 - 86%, the data set also includes the EXOTIC-6 pebble bed with pebbles of 94% density and 10 - 40 μm grain size, pebble-bed smear density of 52.5% and pebble-bed temperature profile of 315 - 425°C. The predicted and measured inventories are 3.45 wppm and 2.3 wppm, respectively. It is also shown in Fig. 4 that the inventories implied by the MOZART transient release data (local temperatures of 270 - 650°C) are bounded by the recommended residency-time approach.

Based on the lessons learned from the Li_2O comparison, some caution must be exercised in using the Li_2ZrO_3 residency time correlation for design applications which may have higher moisture levels than the experiments, particularly at the lower temperatures. Kawamura and Nishikawa [13] studied the adsorption of water vapor for the Li_2ZrO_3/H_2O system at 120 - 400°C and for moisture partial pressures of range 20 - 160 Pa. The adsorbed moisture increased continuously as the temperature was lowered and/or the moisture pressure was increased. Thus, LiOT precipitation does not seem to be an issue for an Li_2ZrO_3 breeding blanket in the range of operating conditions of interest. In order to complete the validation of the residency time approach for Li_2ZrO_3, direct inventory data for samples irradiated at 200 - 300°C and/or data for fundamental mechanisms (e.g., diffusion and desorption) in this range are needed.

Design Application

Tritium inventory calculations are compared in Fig. 5 for layers of Li_2O (TIARA) and Li_2ZrO_3 (residency time) vs. the minimum breeder temperature (T_{min}) with the temperature increase across the breeder, $\Delta T = T_{max} - T_{min}$, shown as a parameter. The tritium generation rate is taken as 184 g/day (Gohar et al. [14] for ITER/EDA) and the peak moisture pressureis assumed to be 10.7 Pa (Billone et al. [15] for the ITER/CDA). The predicted tritium inventories for both breeders and all ΔT cases are relatively small for T > 368°C. For T ≤ 368°C, LiOT precipitation initiates in Li_2O and inventories are predicted to be quite large. However, for Li_2ZrO_3 which does not precipitate out LiOT in this range, the minimum breeder temperature at which the inventory is one-day's-generation (184 g) is 232°C for ΔT = 100°C and < 200°C for ΔT = 300-500°C. Thus, Li_2ZrO_3 has an a distinct advantage with regard to tritium inventory over Li_2O for low temperature operation.

The ITER design described in Ref. 14 includes three outboard and two inboard layers of 10-mm-thick binary-pebble-bed Li_2ZrO_3 with effective smear density of 70%. Each layer is surrounded by layers of beryllium multiplier. The temperature range for the breeder is 272-699°C and the tritium generation rate is 184 g/day. Using the proposed residency time correlation for each layer gives a total tritium inventory of only 24 g. An alternate design has been proposed with two outboard and one inboard layer of 87%-dense sintered-product Li_2O. The ΔT across each breeder layer for this design is much less than the ΔT for the Li_2ZrO_3 pebble-bed. However, the ΔT from coolant to breeder surface is much greater for the Li_2O design in order to maintain T_{min} > 368°C, such that the total ΔT from coolant to breeder centerline is greater for the Li_2O case than for the

Li_2ZrO_3 case. This result, along with the temperature limits for both materials, gives more flexibility to the Li_2ZrO_3 design in accommodating thermal powers greater than the nominal value.

Conclusions

Thermal conductivity correlations for sintered-product Li_2O and Li_2ZrO_3 are reviewed. These correlations are based on data in the temperature and porosity ranges of 200-900°C and 6.6-29.2% for Li_2O and 100-790°C and 18.7-21.1% for Li_2ZrO_3. Using these correlations in a modified Hall and Martin model gives reasonable agreement with data for single-size pebble beds in He with particle porosities of 6.7-25%, packing fractions of 55-62% and particle diameters of 0.5-5.0 mm.

While the Tiara code is recommended for predictions of steady-state tritium inventory in Li_2O, a residency-time correlation is proposed for Li_2ZrO_3. The TIARA code is validated to 20 data points for sintered-product (80-91% dense) Li_2O irradiated at 494-1000°C with tritium generation rates of 3.4-33.0 wppm/day and He purge with ~0-300 Pa of H_2. The Li_2ZrO_3 residency time correlation is validated to 31 data points for sintered-product (73-86% dense) and pebble-bed (about 52% smear density) forms at 315-1044°C with tritium generation rates of 0.38-10.6 wppm/day and purged by He +0.1% H_2. In comparing the thermal and tritium performance of these two breeders, it appears that Li_2ZrO_3 is better than Li_2O for low temperature operation because it is less likely to trap tritium as LiOT precipitates. This makes Li_2ZrO_3 more attractive as a breeder ceramic for low-coolant-temperature machines such as ITER. However, tritium inventory data and/or fundamental mechanistic data are needed to validate tritium inventory predictions for this material at temperatures lower than about 300°C.

References

1. T. Takahashi and T. Kikuchi, J. Nucl. Mater. 91 (1980) 800.

2. P. Gierszewski, Fusion Tech. 23 (1993) 333.

3. R. O. A. Hall and D. G. Martin, J. Nucl. Mater. 101 (1981) 172.

4. M. C. Billone, W. Dienst, T. Flament, P. Lorenzetto, K. Noda and N. Roux, "ITER Solid Breeder Blanket Materials Database," Argonne National Laboratory, ANL/FPP/TM-263, Nov. 1993.

5. H. Yoshida, "Experimental Studies on Blanket in JAERI," ITER Report: ITER-IL-BL-5-0-2, Jan. 1990.

6. M. Dalle Donne and G. Sordon, Fusion Tech. 17 (1990) 597.

7. J. D. Sullivan, C. L. Brayman, R. A. Verrall, J. M. Miller, P. J. Gierszewski and F. Londy, Fusion Eng. & Des. 17 (1991) 79.

8. M. C. Billone, Fusion Eng. & Des. 28 (1995) 313.

9. M. C. Billone, Proc. International Workshop on Ceramic Breeder Blanket Interactions, ed. C. E. Johnson, Los Angeles, June 22-24, 1994, p. 327.

10. H. Kwast, personal communication, ECN-Nucleaire Energie, Feb. 13, 1995.

11. J. P. Kopasz and C. E. Johnson, "performance of Ceramic Breeder materials in the SIBELIUS Experiment," Fourth Symposium on the Fabrication and Properties of Fusion Ceramics, ACSM Meeting, April 1994, to be published in J. Nucl. Mater.

12. R. E. Verrall, "Distribution of Li_2ZrO_3 PIE Data," to be presented at the BEATRIX-II Modelers and Code Developers Working Group Meeting, Tokyo, Oct. 6, 1995.

13. Y. Kawamura and M. Nishikawa, J. Nucl. Mater. 218 (1994) 57.

14. Y. Gohar, M. Billone, A Cardella, W. Dänner, K. Ioki, T. Kuroda, D. Lousteau, P. Lorenzetto, S. Majumdar, R. Mattas, K. Mohri, R. Raffray, Y. Strebkov, H. Takatsu and E. Zolti, "ITER Breeding Blanket Design," to be presented at the 16th IEEE/NPSS Symposium on Fusion Engineering, Sept. 30 - Oct. 5, 1995.

15. M. C. Billone, C. C. Lin, H. Attaya and Y. Gohar, Fusion Tech. 19 (1991)976.

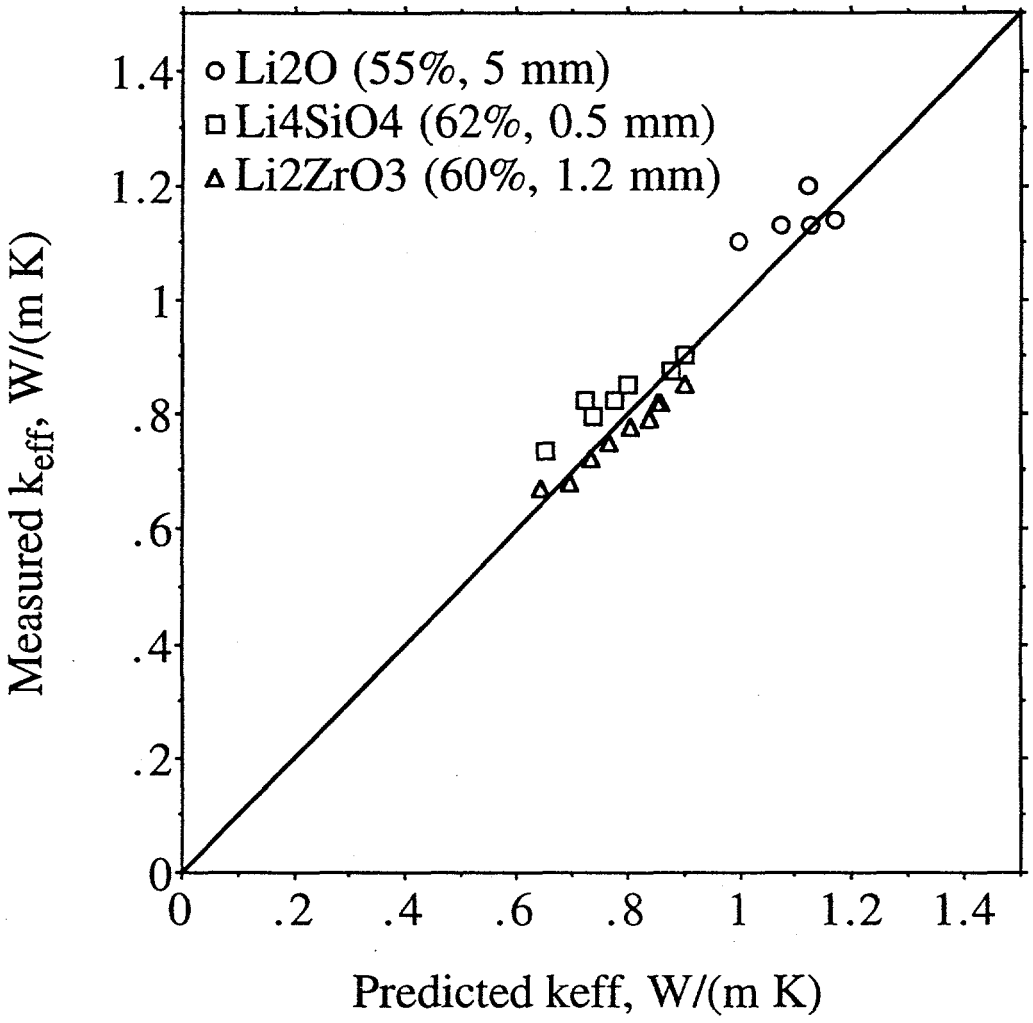

Fig. 1. Predicted vs. measured effective thermal conductivities of single-size packed beds in atmospheric helium. The numbers in parentheses indicate the packing fraction in % and the pebble diameter in mm.

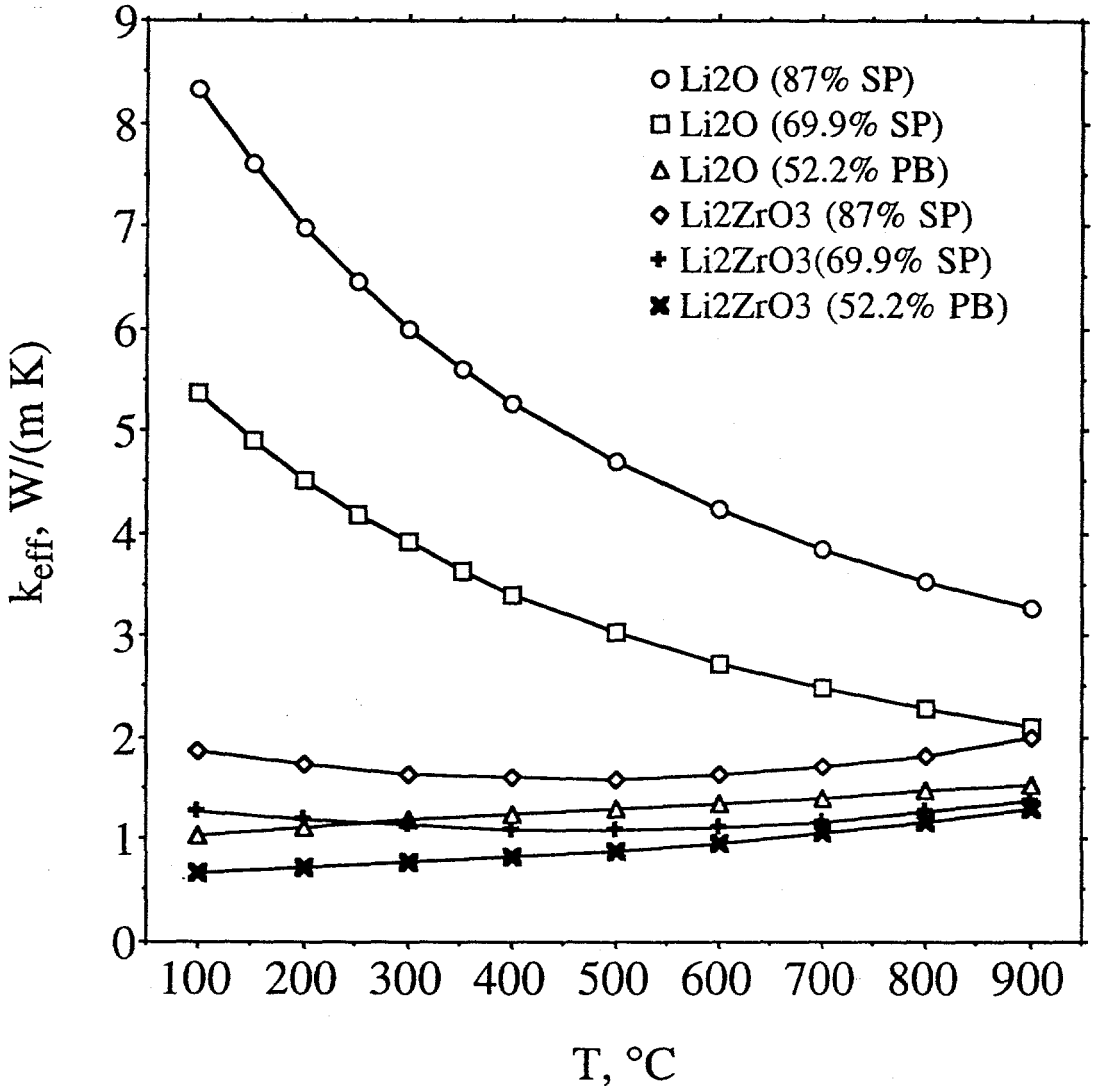

Fig. 2. Predicted effective thermal conductivities (k_{eff}) of sintered product (SP) and pebble bed (PB) forms of Li_2O and Li_2ZrO_3. The numbers in parentheses are smear densities.

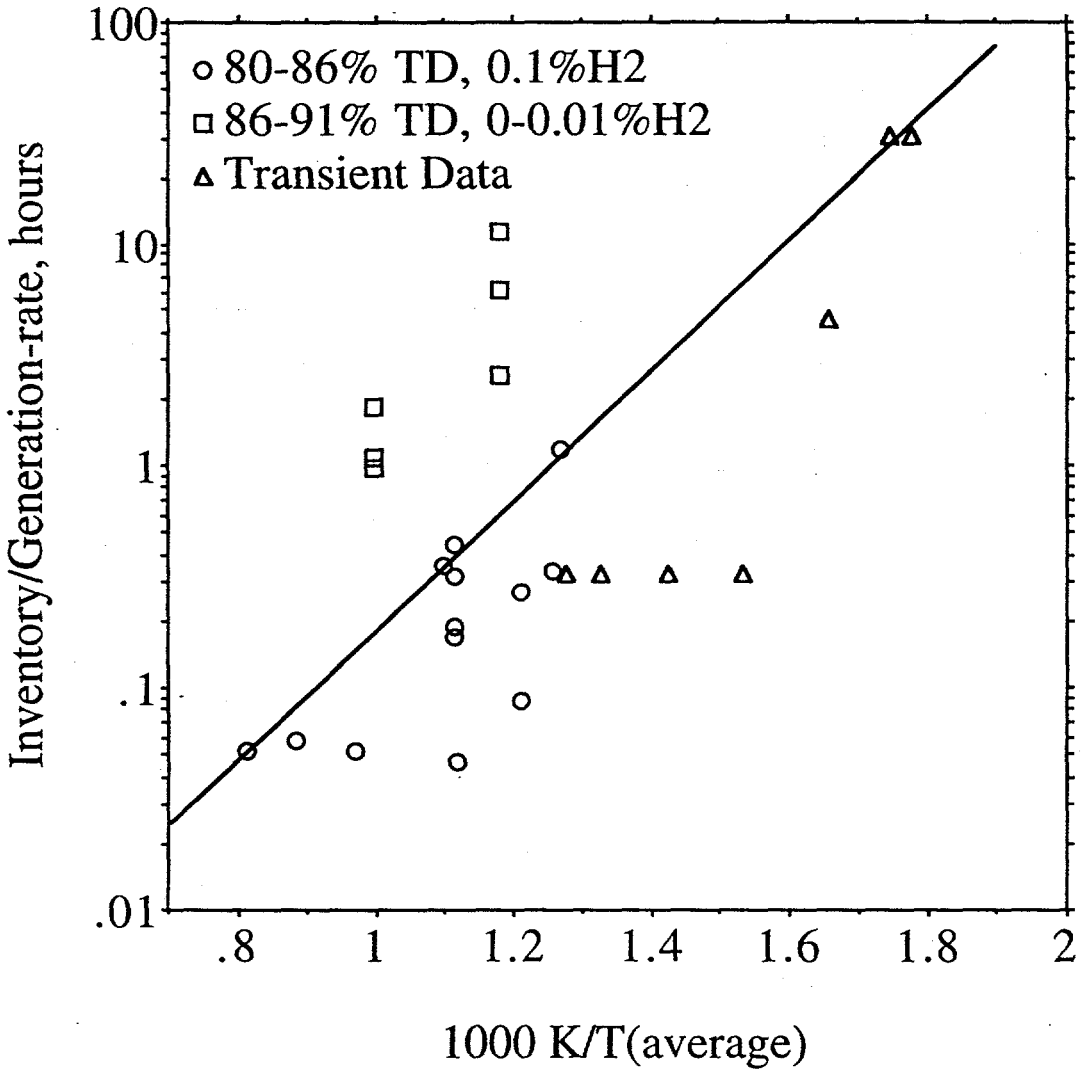

Fig. 3. Tritium residency times for Li_2O determined from post-irradiation tritium inventory measurements as compared to residency times determined from transient tritium release data (e.g. MOZART). The solid line is a recommended design correlation for He + 0.1% H_2 purge, 80-86% density and 5-20 μm grain diameter.

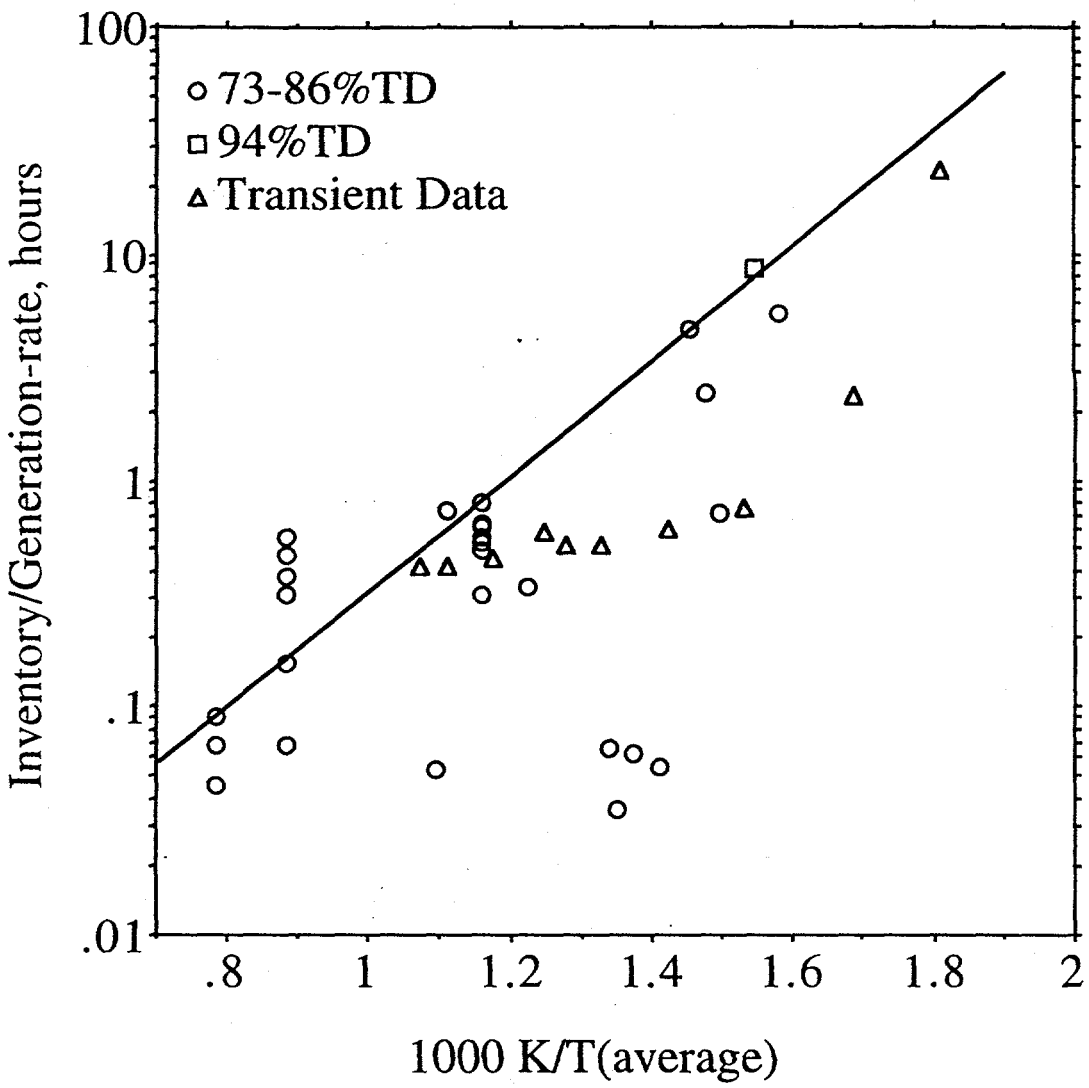

Fig. 4. Tritium residency times for Li_2ZrO_3 determined from post-irradiation tritium inventory measurements as compared to residency times determined from transient tritium release data (e.g. MOZART). The solid line is a recommended design correlation for He + 0.1% H_2 purge, 73-86% density and ≤ 3 μm grain diameter.

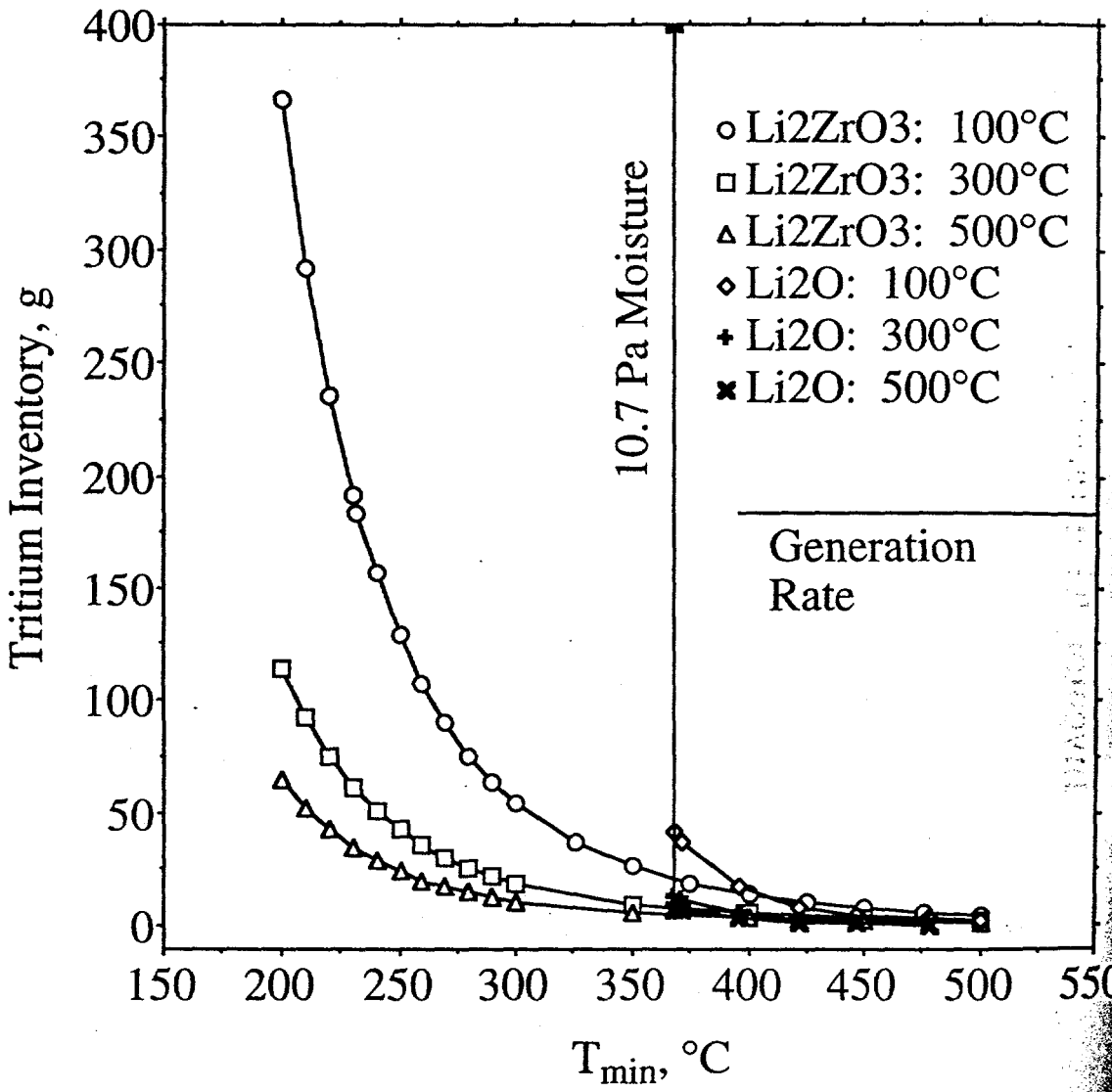

Fig. 5. Predicted tritium inventory in an ITER/EPP driver blanket design composed of Li_2O or Li_2ZrO_3 ceramic breeder. The tritium generation rate is 184 g/day. Results are for temperature increases (Tmax - Tmin) across the breeder layers of 100, 300 and 500°C and a peak moisture pressure of 10.7 Pa.